Sihvola, Ari; Kong, Beibei; Ylä-Oijala, Pasi; Tzarouchis, Dimitrios C; Wallén, Henrik

Scattering, Extinction, and Albedo of Impedance-Boundary Objects

Published in:
URSI Radio Science Letters

DOI:
10.46620/19-0009

Published: 01/01/2019

Document Version
Peer-reviewed accepted author manuscript, also known as Final accepted manuscript or Post-print

Please cite the original version:
Sihvola, A., Kong, B., Ylä-Oijala, P., Tzarouchis, D. C., & Wallén, H. (2019). Scattering, Extinction, and Albedo of Impedance-Boundary Objects. *URSI Radio Science Letters*, *1*. https://doi.org/10.46620/19-0009

Scattering, Extinction, and Albedo of Impedance-Boundary Objects

Ari Sihvola, Beibei Kong, Pasi Ylä-Oijala, Dimitrios C. Tzarouchis, and Henrik Wallén

Abstract – This letter presents results on scattering and absorption behavior of lossy impedance-boundary spheres and cubes. The albedo (the ratio between the scattering and extinction cross sections) of these scatterers turns out to be a very insightful quantity in this respect. The strongly non-linear dependence of albedo on the size of the objects is illustrated and compared to the albedo of dissipative penetrable spheres. The shape of the object seems to have surprisingly little effect on the albedo. Furthermore, the effect of losses on the resonance behavior of small impedance-boundary spheres is analyzed, leading to the observation that the dipolar mode vanishes from the albedo spectrum while higher-order multipoles remain visible. This resembles a similar phenomenon earlier shown to appear in connection with small plasmonic scatterers.

1. Introduction

Material particles and objects form inhomogeneities that disturb the propagation of electromagnetic waves. Wave energy is scattered and possibly absorbed. In this letter, the focus is on scattering by objects which are characterized by the boundary condition on their surface. In the electromagnetics literature, a wide variety of boundary conditions has been studied, both theoretically [1] and as useful approximations [2, 3]. In the following, we will focus on scattering objects with the so-called impedance boundary condition.

The impedance boundary condition (IBC) is a condition between the tangential components of electric ($\mathbf{E}$) and magnetic ($\mathbf{H}$) field vectors at a boundary. A relation between two two-dimensional vectors is in general a dyadic, and hence the impedance boundary condition has to be described by four scalars. Formally, the impedance condition is written

$$\mathbf{E}_t = \overline{\overline{\mathsf{Z}}}_s \cdot (\mathbf{n} \times \mathbf{H}_t) \tag{1}$$

where the tangential electric and magnetic fields at the boundary with normal unit vector $\mathbf{n}$ are

$$\mathbf{E}_t = -\mathbf{n} \times (\mathbf{n} \times \mathbf{E}), \quad \mathbf{H}_t = -\mathbf{n} \times (\mathbf{n} \times \mathbf{H}) \tag{2}$$

Here the surface impedance dyadic $\overline{\overline{\mathsf{Z}}}_s$ is two-dimensional, in the plane perpendicular to $\mathbf{n}$ (in other words $\mathbf{n} \cdot \overline{\overline{\mathsf{Z}}}_s = 0$ and $\overline{\overline{\mathsf{Z}}}_s \cdot \mathbf{n} = 0$), which here operates on the electric and magnetic fields.

In the simplest case, the dyadic $\overline{\overline{\mathsf{Z}}}_s$ is a multiple of the unit dyadic, whence the boundary condition simplifies to

$$\mathbf{E}_t = Z_s \, \mathbf{n} \times \mathbf{H}_t \tag{3}$$

This isotropic IBC is also known in the literature as the Leontovich boundary condition [4, 5].

This surface impedance model can be particularly interesting in a multitude of ways. Good conductors are often treated as isotropic IBC surfaces. Also, general IBC models have connections with *metasurfaces* which are presently under active research interest [6]. The properties of metasurfaces are usually characterized via a sheet impedance. This type of approach has been used to introduce concepts such as mantle cloaking [7, 8].

Furthermore, IBC models can be used as equivalent descriptions for real phenomena, such as the plasmonic and dielectric resonances in a sphere [9]. In addition, more exotic cases of impedance boundary conditions can be potentially used towards unexplored regions of electromagnetic wave manipulation. A fascinating example is the PEMC (perfect electromagnetic conductor) boundary and medium [10] with connections to axion electrodynamics [11] and topological insulators [12].

In our previous studies [13], we have analyzed interesting resonance spectra of spheres with lossless impedance boundary. In this letter—which is an expanded study of [14]—we analyze the scattering by IBC objects whose (isotropic) surface impedance is dissipative.

2. Albedo

A dissipative scatterer perturbs and therefore attenuates a propagating wave in two ways: by scattering and by absorbing electromagnetic energy. For finite scatterers, measures for these two contributions are the scattering efficiency $Q_{\rm sca}$ and the absorption efficiency $Q_{\rm abs}$, with the sum of the two being the extinction efficiency $Q_{\rm ext} = Q_{\rm sca} + Q_{\rm abs}$ [15]. In the following analysis, a useful quantity is the albedo A of the scatterer. Albedo (whiteness) is the ratio between scattering and extinction cross sections (or efficiencies).

$$A = \frac{Q_{\rm sca}}{Q_{\rm ext}}. \tag{4}$$

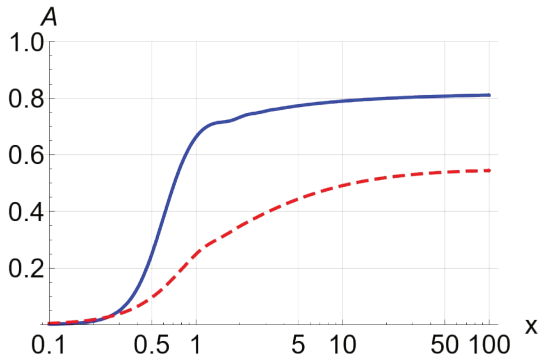

Figure 1: The albedo of a lossy IBC-boundary sphere with $Z_s = 10\eta_0$ (solid blue) and $Z_s = \eta_0$ (dashed red) as function of electrical size parameter x.

Albedo has a value between zero (for totally absorbing body) and unity (for completely scattering object). In passing, we may note that with active scatterers, these limits for the albedo can be overcome.

3. Lossy sphere

Let us start by the scattering and absorption characteristics of a lossy IBC sphere, defined by two parameters: its electrical size $x = 2\pi a/\lambda$ and the (possibly complex) surface impedance $Z_s = R_s + \mathrm{j}X_s$. The time-harmonic notation of $\exp(\mathrm{j}\omega t)$ is followed, the radius of the sphere is a, and λ is the wavelength.

Figure 1 displays how the albedo of a lossy IBC sphere varies when the size parameter changes. From a very low albedo it increases with size, with a very non-linear speed of increase. Furthermore, as expected, a sphere with surface resistance matching the free-space impedance ($Z_s = \eta_0$) has a lower albedo than one with impedance contrast. Figure 2 takes a closer look into the small-size regime, also called the Rayleigh regime. (In electromagnetic scattering, the Rayleigh regime is conspicuous of the strong, fourth-order dependence of the scattering on the relative size [16].) A somewhat counterintuitive observation is that for very small spheres, the albedo of a sphere with surface impedance $Z_s = \eta_0$ is higher than that of the impedance-contrast sphere ($Z_s = 10\eta_0$), as shown in Figure 2. However, at the crossover point ($x \approx 0.25$) the albedos are already quite low ($A \approx 0.028$), and the inversion in the albedo behavior is hence more of an academic interest.

For increasing size of the sphere, the increase of the albedo starts to saturate, meaning that the mutual share of scattering and absorption remain unchanged.

It is of interest to compare this albedo behavior to that of a penetrable sphere. Figure 3 shows the albedo of a lossy dielectric sphere as its electrical size increases.

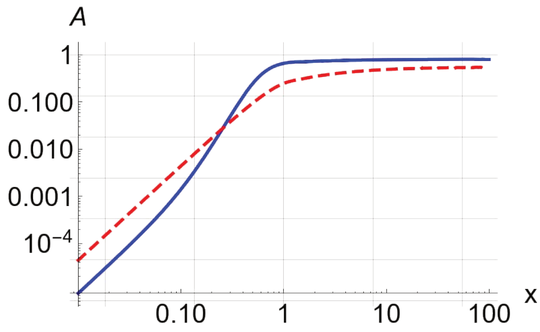

Figure 2: A logarithmic view on the albedo of IBC spheres: $Z_s = 10\eta_0$ (solid blue) and $Z_s = \eta_0$ (dashed red) as function of the electrical size parameter x.

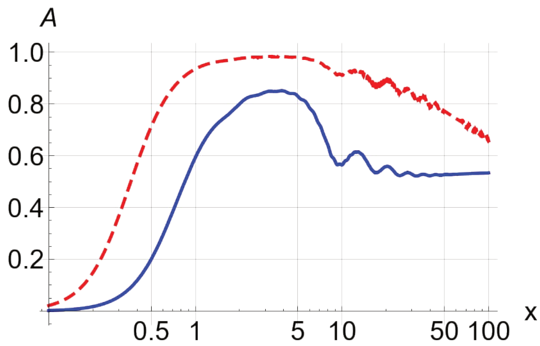

Figure 3: The albedo of a penetrable lossy sphere with relative permittivity $\varepsilon_r = 2 - \mathrm{j}0.1$ (solid blue) and $\varepsilon_r = 2 - \mathrm{j}0.01$ (dashed red) as function of the electrical size parameter x.

Here we can observe that although the Rayleigh regime looks similar to that of the IBC sphere, the increase of the albedo is not continuous: it is rather non-linear, and it is worth paying attention to the maximum albedo value in the plot for size parameter value around $x = 4$.

In the computations in Figures 1–3, the change in the size parameter x can represent the variation in absolute size, frequency, or a combination of them. However, the impedance Z_s and the permittivity ε were assumed constant throughout the range of x.

4. Effect of scatterer shape

How do these observations on the albedo behavior depend on the shape of the scatterer? To have insight on this, we compute the albedo of a cube with a lossy isotropic surface impedance. The computations have been done using the surface integral equation method based on the electric field integral equation (EFIE) [17]. Figure 4 shows how the albedo increases as function of the size parameter, for the two surface impedance values

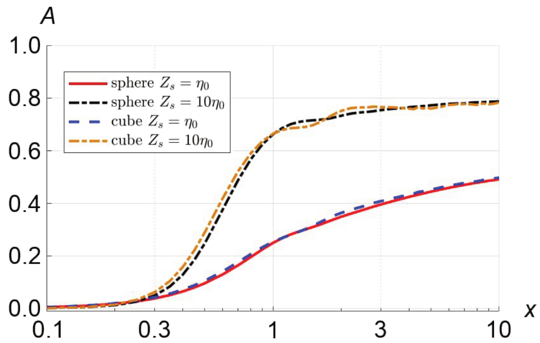

Figure 4: The albedo of a lossy IBC-boundary cube with $Z_s = 10\eta_0$ (solid blue) and $Z_s = \eta_0$ (dashed orange) as function of the electrical size parameter x.

$Z_s = \eta_0$ and $10\eta_0$. Here the size parameter x for the IBC cube is defined as that of the size parameter of an equivolume sphere.

It is rather surprising how similar the behaviors of the two albedo curves of the sphere and the cube are in Figure 4. One can, however, observe a slight oscillation in the albedo curve of the cube while the corresponding behavior of the sphere shows a more smooth increase with x.

Another result from our numerical study of IBC cubes is that for a given size and surface impedance, the albedo of the cube depends neither on the incidence angle nor the polarization of the incident wave vector.

5. Multipolar peculiarities

The scatterers in the previous section were very dissipative. Consider next low-loss IBC scatterers. The fascinating message of our previous studies [13] was that small *lossless* ICB scatterers can support strong multipolar resonances analogously with plasmonic nanoparticles. Does this phenomenon leave its marks on the albedo? To answer this, we have computed the response of low-loss IBC spheres with varying parameters. Figure 5 shows the scattering and absorption efficiencies of spheres with size parameter less than one and with capacitive but lossy surface impedance $Z_s = (0.01 - \mathrm{j}0.2)\eta_0$. There, a fairly strong resonance can be seen for size parameter values $x \approx 0.2$, and weaker ones for $x \approx 0.4$ and 0.6.

However, the resonances take a different profile in the scattering and absorption curves in Figure 5. This fact becomes very clearly illustrated when the albedo is plotted as a function of the size parameter, as is done in Figure 6. For the low-loss sphere (solid blue curve), the albedo curve is practically totally smooth through the dipole ($x \approx 0.2$) but the quadrupole ($x \approx 0.4$) has a strong dip, likewise the octopole ($x \approx 0.6$), and even at a higher multipole ($x \approx 0.8$), a dip can be distinguished. Hence,

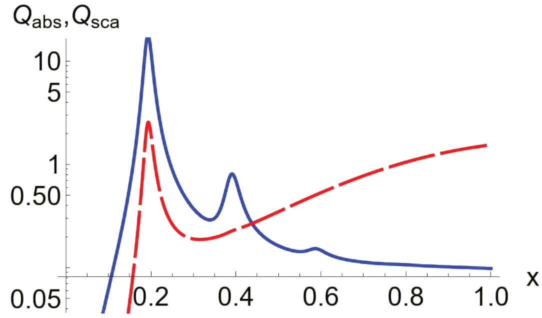

Figure 5: The absorption (solid blue) and scattering (dashed red) efficiencies of a small lossy IBC sphere as function of the electrical size parameter x. The surface impedance is $Z_s = (0.01 - \mathrm{j}0.2)\eta_0$.

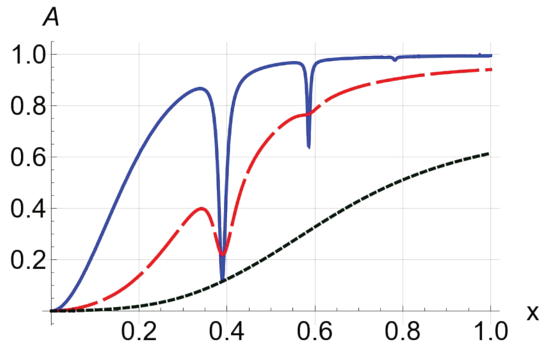

Figure 6: The albedo of a small lossy IBC sphere as function of the electrical size parameter x. The surface impedance is $Z_s/\eta_0 = 0.001 - \mathrm{j}0.2$ (solid blue), $0.01 - \mathrm{j}0.2$ (dashed red), and $0.1 - \mathrm{j}0.2$ (dotted green).

at these higher-order multipoles, the absorptive character of the IBC particle dominates over the scattering power. The other curves in Figure 6 show that even a fairly small value of the real part in the surface impedance will wash out the resonance structure in the albedo curves. But unlike in the case for the smooth albedo over the dipole region, this ultimate flattening is due to the fact that both the scattering and absorption cross sections lose their multipolar peaks, and not due to the qualitative difference in the scattering and absorption curves.

The behavior of the resonances in Figures 5 and 6 resembles the one which has been observed earlier in connection with nanoplasmonics [18, 19]. For small plasmonic (negative-permittivity) scatterers, the quadrupole has a distinct profile in the albedo maps, while the dipole is practically invisible. Admittedly also differences exist: the resonances in electrically small IBC spheres (which appear for capacitive surface reactances [13]) are of magnetic resonance type, while in the case of small plasmonic spheres, the localized surface plasmons are all due to electric multipoles [18].

6. Conclusion

The scattering, absorption, and extinction responses of impedance-boundary objects depend on their size and shape, in addition to their complex surface impedance. Analysis of the response functions, illustrated in this letter, leads to several interesting conclusions, in particular in the albedo behavior. One of these observations is the surprising similarity of the albedos of sphere and cube, suggesting on insensitivity of the albedo of the shape of an IBC scatterer. Also, we could note the strong difference in the manner how the multipolar resonances appear in the albedo spectrum: the dipole mode is invisible while the higher-order modes can be distinguished clearly as dips in the albedo curve.

7. References

1. I.V. Lindell and A.Sihvola: *Boundary Conditions in Electromagnetics*, New York, Wiley/IEEE Press, 2020.
2. D.J. Hoppe and Y. Rahmat-Samii, *Impedance Boundary Conditions in Electromagnetics*, Washington, D.C., Taylor and Francis, 1995.
3. T.B.A. Senior and J.L. Volakis, *Approximate Boundary Conditions in Electromagnetics*, London, IEE, 1995.
4. A.N. Shchukin, *Propagation of Radio Waves*, Moscow, Svyazizdat, 1940.
5. M.A. Leontovich, "Methods of Solution for Problems of Electromagnetic Wave Propagation along the Earth Surface," *Bulletin of the Academy of Sciences of USSR, Physics Ser.*, **8**, 1, 1944, pp. 16-22.
6. O. Quevedo-Teruel et al., "Roadmap on Metasurfaces," *Journal of Optics*, **21**, 7, 2019, p. 073002.
7. A. Alù, "Mantle Cloak: Invisibility Induced by a Surface," *Physical Review B*, **80**, 24, 2009, p. 245115.
8. P.-Y. Chen and A. Alù, "Mantle Cloaking using Thin Patterned Metasurfaces," *Physical Review B*, **84**, 20, 2011, p. 205110.
9. D.C. Tzarouchis, H. Wallén, P. Ylä-Oijala, and A. Sihvola, "Can a Dielectric Sphere Emulate the Behavior of a Surface Impedance Sphere?" 2019 URSI International Symposium on Electromagnetic Theory, San Diego, CA, paper D08–2.
10. I.V. Lindell and A.H. Sihvola, "Perfect Electromagnetic Conductor," *Journal of Electromagnetic Waves and Applications*, **19**, 7, 2005, pp. 861-869.
11. F.W. Hehl, "Axion and Dilaton + Metric Emerge Jointly from an Electromagnetic Model Universe with Local and Linear Response Behavior," *International Journal of Modern Physics D*, **25**, 11, 2016, p. 1640015.
12. J. Yu, J. Zang, and C.-X. Liu, "Magnetic Resonance Induced Pseudoelectric Field and Giant Current Response in Axion Insulators," *Physical Review B*, **100**, 2019, p. 075303.
13. A. Sihvola, D.C. Tzarouchis, P. Ylä-Oijala, H. Wallén, and B.B. Kong, "Resonances in Small Scatterers with Impedance Boundary," *Physical Review B*, **98**, 2018, p. 235417.
14. A. Sihvola, D.C. Tzarouchis, P. Ylä-Oijala, H. Wallén, and B. Kong: "Scattering, Extinction, and Albedo of Impedance-Boundary Spheres," 2019 URSI International Symposium on Electromagnetic Theory, San Diego, CA, paper E05–2.
15. C.F. Bohren and D.R. Huffman, *Absorption and Scattering of Light by Small Particles*, New York, Wiley, 1983.
16. M. Born and E. Wolf, *Principles of Optics*, New York, Pergamon Press, 1970.
17. P. Ylä-Oijala, B. Kong, and S. Järvenpää, "Modeling of Resonating Closed Impedance Bodies With Surface Integral Equation Methods," *IEEE Transactions on Antennas and Propagation*, **67**, 1, January 2019, pp. 361-368.
18. D.C. Tzarouchis, P. Ylä-Oijala, and A. Sihvola, "Study of Plasmonic Resonances of Platonic Solids," *Radio Science*, **52**, 12, 2017, pp. 1450-1457.
19. D.C. Tzarouchis, "Resonant Scattering Particles — Morphological Characteristics of Plasmonic and Dielectric Resonances on Spherical, Superquadric, and Polyhedral Inclusions," Aalto University publication series, DOCTORAL DISSERTATIONS, 38/2019, March 2019. `https://aaltodoc.aalto.fi/handle/123456789/36611`

The Authors A.S., B.K., P.Y-O., and H.W. are with Aalto University, Department of Electronics and Nanoengineering, 00076 Aalto, Finland; e-mail: firstname.lastname@aalto.fi, and D.C.T. is with University of Pennsylvania, 19104 Philadelphia, USA; e-mail: dtz@seas.upenn.edu.